

# Effect of Film Cooling/Regenerative Cooling on Scramjet Engine Performances

Takeshi Kanda,\* Goro Masuya,† Fumiei Ono,‡ and Yoshio Wakamatsu§  
 National Aerospace Laboratory, Kakuda Research Center, Kimigaya, Kakuda, Miyagi 981-15, Japan

Film cooling was modeled to allow performance prediction of scramjet engine design. The model was based on experimental results of the compressible mixing layer for the vicinity of the injection slot, and on analytical results of the turbulent boundary layer in the region far from the slot. The film cooling model was integrated with a quasi-one-dimensional scramjet performance prediction model. In an engine employing a combination of film cooling and regenerative cooling, coolant flow rate of the engine slightly exceeded the stoichiometric flow rate, even at high flight Mach numbers, and had the best specific impulse and system pressure performances. These advantages were achieved by an increase in the volume flow rate and a decrease in the velocity difference between the main flow and the coolant, both due to an increase in the film coolant temperature. The effective cooling system with a combination of film cooling and regenerative cooling was also advantageous with regard to avoidance of excess cooling of the engine wall.

## Nomenclature

$a$  = sound velocity  
 $b$  = power law index of turbulent boundary-layer growth rate  
 F.C. = film cooling  
 $f$  = compressibility effect in growth rate of mixing layer  
 $h$  = injection slot height  
 $I_{sp}$  = specific impulse  
 $L$  = length  
 $l$  = circumferential length of combustor, height of inlet at the entrance  
 $M$  = Mach number  
 $\bar{M}$  = convective Mach number  
 $\dot{m}$  = mass flow rate  
 $P_0$  = total pressure  
 $q$  = dynamic pressure  
 $R$  = gas constant  
 R.C. = regenerative cooling  
 $T$  = temperature  
 $T_0$  = total temperature  
 $u$  = velocity  
 $\bar{u}$  = convection velocity  
 $x$  = distance from injection slot  
 $\gamma$  = ratio of specific heats  
 $\delta$  = mixing-layer thickness  
 $\eta$  = film cooling efficiency defined in Fig. 1  
 $\theta$  = external nozzle angle  
 $\lambda$  = mass flux ratio  
 $\rho$  = density  
 $\phi$  = equivalence ratio

## Subscripts

$A$  = position where mixing layer reaches wall  
 $a$  = adiabatic

C.C. = combustor  
 $c$  = coolant  
 $g$  = hot gas  
 H<sub>2</sub> = hydrogen  
 I.N. = internal nozzle  
 $m$  = main flow  
 ref = reference condition  
 st = stoichiometric  
 $w$  = wall  
 $0$  = incompressible  
 $\infty$  = flight condition

## I. Introduction

THE scramjet is a candidate for use as the engine of the aerospace plane. When the aerospace plane flies with a scramjet at very high speed, total temperature in the engine becomes very high and heat load becomes very great, necessitating employment of an effective thermal protection system. Regenerative cooling and film cooling appear to be useful techniques for such a cooling system.

According to previous studies,<sup>1–4</sup> in a regeneratively cooled scramjet, coolant flow rate exceeds stoichiometric flow rate in the high flight Mach number region beyond about 10, and the engine system pressure becomes extremely high. Therefore, specific impulse is degraded with excess fuel flow rate and with a high level of turbine exhaust gas from the fuel supply system.<sup>4</sup> At the same time, the engine must be strongly made, and thus becomes heavy.

Supersonic film cooling has been studied by various researchers.<sup>5–12</sup> The benefits of applying film cooling to a scramjet engine, other than cooling itself, have been mentioned in many reports,<sup>5,6</sup> i.e., reduction of skin friction and thrust augmentation. There have been, however, few quantitative studies on scramjet engine performances with film cooling, mainly because of the difficulty of modeling film cooling. One model of film cooling is the turbulent boundary-layer model.<sup>13,14</sup> It was originally introduced for subsonic film cooling, and is the most popular model. It adopts the growth rate of the turbulent boundary layer. This model can predict the decay tendency of film cooling efficiency far downstream from the injection slot. It has been applied to predict the flow condition near the slot with several combinations of gas properties as parameters, e.g., density, heat capacity, etc. These combinations, however, do not seem to be so well-grounded physically. Moreover, the boundary layer and the coolant are separated near the injection slot, and it does not seem reasonable

Received April 12, 1993; revision received Feb. 1, 1994; accepted for publication Feb. 17, 1994. Copyright © 1994 by the American Institute of Aeronautics and Astronautics, Inc. All rights reserved.

\*Senior Researcher, Ramjet Propulsion Research Division. Member AIAA.

†Head, Ramjet Aerodynamics Section, Ramjet Propulsion Research Division. Member AIAA.

‡Researcher, Ramjet Structure Section, Ramjet Propulsion Research Division.

§Head, Ramjet Structure Section, Ramjet Propulsion Research Division. Member AIAA.

to apply the model for the vicinity of the slot. In another model, the main flow and film coolant are separated completely.<sup>15</sup> It does not seem to simulate the flow condition in film cooling far downstream of the slot. There have been few investigations employing CFD.<sup>6</sup> Investigation with CFD can simulate three-dimensional effects, but it is time-consuming and expensive, and necessitates many calculations to clarify the tendency of film cooling.

In the present study, we constructed a new film cooling model and confirmed it to be consistent with experimental results. We then used it to predict scramjet engine performances and compared predicted performances of several cooling systems in the range of flight Mach number from 8 to 24 along the flight path of a flight dynamic pressure of 100 kPa.

## II. Film Cooling Model

According to experimental results,<sup>5-12</sup> there is a relation between film cooling efficiency defined in Fig. 1 and the distance from the exit of a coolant injection slot. Cooling efficiency  $\eta$  and the distance  $x/(h \cdot \lambda)$ , are plotted with logarithm scales. In previous film cooling models, no attempt was made to model the flow between the slot exit and position  $A$  in Fig. 1, where the efficiency is around unity. Rather, prediction of  $A$  was attempted by extension of the turbulent boundary-layer model. This length from the slot exit to  $A$ ,  $x_A$  in Fig. 1, is shorter than the length of the effective region of film cooling,  $x_1$  in Fig. 1.  $x_1$  is the length from the slot exit to the position where the adiabatic wall temperature is  $T_{aw,1}$ . The prediction of  $A$  is, however, very important because the effective length of film cooling  $x_1$  greatly differs due to the small difference of  $A$ . Therefore the prediction of position  $A$  must be included in a model of film cooling.

The flow conditions of the coolant are completely independent of the main flow in the vicinity of the injection slot, and the coolant and the main flow mix with each other gradually. This mixing seems to resemble the turbulent mixing layer.<sup>16-18</sup> Thus, an experimental equation of the turbulent mixing layer was used to predict position  $A$ . The boundary layer of the main flow seems to completely take in the film coolant far downstream of the injection slot, and this is the basis of the turbulent boundary-layer model. In our model, the flow region of film cooling was divided into two parts: 1) a mixing-layer region near the injection slot and 2) a turbulent boundary-layer region far from the slot. The schematic diagram of the model is shown in Fig. 2. At position  $A$ , the mixing layer is assumed to reach the wall in the model, and the concept of the mixing layer was applied from the injection slot exit to  $A$ . The thickness of the boundary layer on the wall under the coolant was much thinner than the slot height

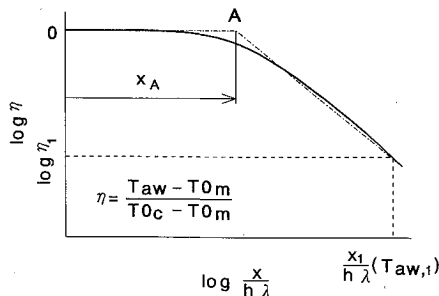


Fig. 1 Schematic of film cooling efficiency.

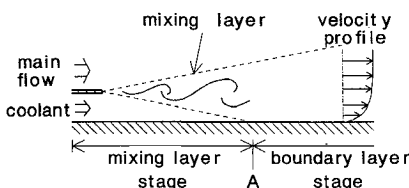


Fig. 2 Schematic of film cooling model.

and also thinner than the thickness of the mixing layer, so the effect of the coolant side boundary layer was neglected. The idea of turbulent boundary layer was applied to the area downstream of position  $A$ . In this model, static pressure of the coolant was assumed to be the same as that of the main-stream at the slot exit.

### A. Mixing Layer Region

In this region, effects of density ratio, velocity ratio, and compressibility on the growth rate of the mixing layer are taken into account, following the experimental equation of Papamoschou and Roshko<sup>17</sup>:

$$\frac{d\delta}{dx} = \left(\frac{d\delta}{dx}\right)_0 \cdot f(\overline{M}_m) \quad (1)$$

The effect of  $f$  can be expressed as a function of  $\overline{M}$ . Definition of the convective Mach number is as follows:

$$\overline{M}_m = [(u_m - \bar{u})/a_m] \quad (2)$$

$\bar{u}$  becomes as follows when  $\overline{M}_m$  and  $\overline{M}_c$  are not very large, and  $\gamma$  and  $\gamma_c$  are not greatly different<sup>17</sup>:

$$(\bar{u}/u_m) = \frac{1 + (u_c/u_m)\sqrt{(\rho_c/\rho_m)}}{1 + \sqrt{(\rho_c/\rho_m)}} \quad (3)$$

In this model, the empirical equation of Dimotakis<sup>18</sup> was used to predict the effect of compressibility:

$$f(\overline{M}_m) = (1 - f')\exp(-3\overline{M}_m^2) + f' \quad (4)$$

$f'$  is the value of the compressibility effect, and it is about 0.2 when the convective Mach number is very large. The growth rate of the mixing layer in incompressible heterogeneous flow can be expressed as follows<sup>17</sup>:

$$\left(\frac{d\delta}{dx}\right)_0 = 0.14 \frac{[1 - (u_c/u_m)][1 + \sqrt{(\rho_c/\rho_m)}]}{1 + (u_c/u_m)\sqrt{(\rho_c/\rho_m)}} \quad (5a)$$

$$= 0.14/[1 + (M_c/M_m)\sqrt{(\gamma_c/\gamma_m)}] \times [1 - (M_c/M_m)\sqrt{(\gamma_c/\gamma_m)} - A\sqrt{(T0_c/T0_m)} + B\sqrt{(T0_m/T0_c)}] \quad (5b)$$

Here

$$A = \frac{M_c}{M_m} \sqrt{\frac{1 + [(\gamma_m - 1)/2]M_m^2}{1 + [(\gamma_c - 1)/2]M_c^2}} \sqrt{(\gamma_c/\gamma_m)(R_c/R_m)}$$

$$B = \sqrt{\frac{R_m}{R_c} \frac{1 + [(\gamma_c - 1)/2]M_c^2}{1 + [(\gamma_m - 1)/2]M_m^2}}$$

The distance of the mixing layer region indicated by  $x_A$  in Fig. 1 is as follows with the assumption that the mixing layer grows symmetrically both in main flow and in coolant:

$$x_A = h \left/ \left( \frac{1}{2} \frac{d\delta}{dx} \right) \right. \quad (6)$$

### B. Turbulent Boundary-Layer Region

Hartnett and other researchers assumed that there was a well-developed boundary layer far downstream from the injection slot of the film coolant, and showed that the film cooling efficiency was proportional to  $[x/(h \cdot \lambda)]^{-4/5}$  in an incompressible flow when the 1/7 power law was used as the velocity profile in the turbulent boundary layer.<sup>13,14</sup> Dependence on the distance  $x$  is not changed in the compressible-

incompressible transformation,<sup>19</sup> and so the film cooling efficiency is assumed to be also proportional to  $x^{-4/5}$  in a compressible flow in this study. The position  $x_1$  can be estimated as follows:

$$x_1 = x_A \left( \frac{T_{O_m} - T_{O_c}}{T_{O_m} - T_{aw,1}} \right)^{5/4} \quad (7)$$

With Eq. (6)

$$x_1 = \left[ h / \left( \frac{1}{2} \frac{d\delta}{dx} \right) \right] \left( \frac{T_{O_m} - T_{O_c}}{T_{O_m} - T_{aw,1}} \right)^{5/4} \quad (8)$$

### C. Comparison with Experimental Results

Figure 3 shows a comparison of position  $x_1$  between film cooling experimental results<sup>7-9,12,20,21</sup> and those by Eq. (6). Convective Mach numbers of the experimental results were from 0 to 1.4. The broken lines have inclinations of two and one-half, respectively. Most of the experimental data, except the solid symbols, exist between the broken lines. In the experiments indicated by the solid symbols, velocity differences between the main flow and the coolant were within about 10% of the main flow velocity. As can be seen in Eq. (5), this model predicts a very low growth rate and a very large value of  $x_A$  when the velocity difference is small. In this case, however, other physical phenomena seem to be dominant in mixing.

Figure 4 is a histogram, showing results of a number of experiments on a specified inclination index of decay of film cooling efficiency<sup>8-12,20,21</sup> (see Fig. 1). The inclination of film cooling efficiency by the analysis shifts according to the power law of velocity distribution. Most of the experimental results are around  $-0.7$ , while  $-0.8$  was analytically predicted. So the  $-0.8$  power was adopted in this study.

### D. Problems of this Film Cooling Model

Adoption of the idea of the free shear layer has been rejected by some researchers due to such factors as lack of observation of large-scale structure, and the thick boundary layer of the main flow.<sup>7</sup> We, however, conceive that we can

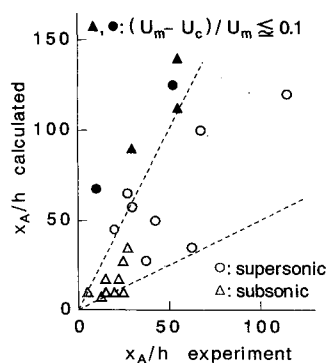


Fig. 3 Comparison between experiments and calculation—length of mixing layer region.

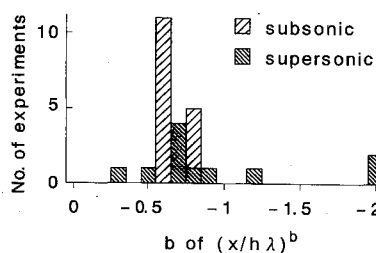


Fig. 4 Comparison between experiments and calculation—decay of film cooling efficiency.

predict the film cooling performance with this model fairly well due to the consistency of theoretical findings with experimental results shown above. In this film cooling model, there are several problems to be solved or modification to be made as follows:

1) Influence of shock impingement: There are several experimental results that show that shock impingement degrades the effect of film cooling drastically.<sup>10,11</sup> However, there are no clear criteria of the influence on film cooling.<sup>22</sup> The effect of the shock impingement is a state-of-the-art research theme.

2) Wall influence on growth rate of the mixing layer: It has been reported that the growth rate is enhanced by the wall.<sup>23</sup> The influence of growth rate on engine performances will be mentioned in the section on simulation results.

3) Mainstream boundary layer: According to one report, shear layer by slot injection begins to have the character of the free shear layer apart from the injector exit with the distance of 25 times of the thickness of the main stream boundary layer.<sup>7</sup> If the boundary layer of the main flow obstructs the growth of the shear layer, the film cooling efficiency may increase.

4) Static pressure distribution: In a scramjet engine, pressure is not uniform. It has been reported that the static pressure gradient of the main flow affects the growth rate of the mixing layer.<sup>24</sup>

5) Static pressure difference at the slot exit: The static pressure of the coolant usually differs from that of the main flow at the exit of the injection slot. Increase of the film coolant injection pressure has been found to increase film cooling efficiency,<sup>10</sup> but the static pressure difference creates shock waves and expansion waves, which will disturb the main flow, the coolant, and the mixing layer. This effect is now being researched.

## III. Simulation Method

### A. Scramjet Engine Schematic Diagram

We compared engine performances among three cooling systems: a) film cooling only, b) regenerative cooling only, and c) a combination of film cooling and regenerative cooling. Schematics of these systems are shown in Fig. 5. In all three engines, coolant was the same fluid as the propellant, i.e., hydrogen. In the engine with only film cooling, the engine was cooled with cold hydrogen, and the cold fuel was injected into the combustor at stoichiometric ratio to the airflow. In the regeneratively cooled engine, the fuel was used to cool the engine. The fuel was heated to several hundred Kelvin. After regenerative cooling, it was injected into the combustor

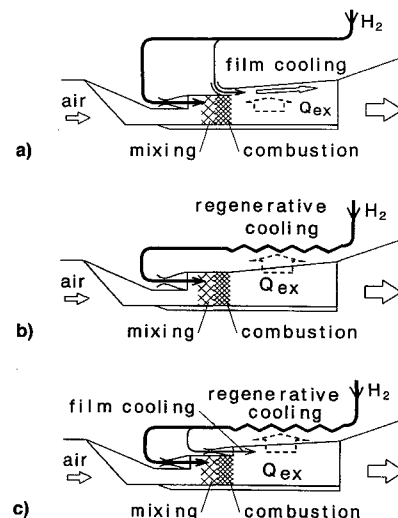


Fig. 5 Scramjet engine schematics: a) film cooling only, b) regenerative cooling only, and c) combination of film cooling and regenerative cooling.

parallel to the air. The flow rate of the fuel injected into the combustor was at least stoichiometric. In the engine with a combination of film cooling and regenerative cooling, fuel cooled the engine regeneratively. Subsequently, part of the heated fuel was injected into the engine as film coolant. The rest of the fuel, which was stoichiometric, was injected into the combustor. In the engine with a combination of film cooling and regenerative cooling, the flow rate of the film coolant was at least 1% of the stoichiometric flow rate in every operation. Both in the engine with only film cooling and in that with a combination of film cooling and regenerative cooling, injection slots of film coolant were set at two positions, i.e., 1) at the entrance of the combustor, and 2) at the middle of the combustor/internal nozzle.

To simplify the simulation, the engine was divided into several components, i.e., an inlet, a fuel injector, a combustor/internal nozzle, a cooling jacket, and an external nozzle. The external nozzle was a part of the surface of an aerospace plane.

The fuel injector of the regeneratively cooled engine was designed at a flight Mach number of 14 and at a fuel supply pressure of 10 MPa. The supply pressure was roughly the same as the pressure at the fuel pump exit. In the other two engines, the same fuel injector was used. The fuel was injected with sonic velocity into the combustor in all the engines.

### B. Engine Configuration

The model engine dimensions, as shown in Fig. 6, resembled those of a previous investigation.<sup>2</sup> The cross section of the inlet at the entrance was the same as that of the internal nozzle at the exit, i.e., 6 m<sup>2</sup>. The projected cross section of the external nozzle at its exit was twice that of the internal nozzle at its exit. The angle of  $\theta$  was 10 deg. The contraction ratio of the inlet was five. The wall thickness of the combustor/internal nozzle was 1 mm. The diameter of the cooling tubes was 10 mm.

### C. Assumptions and Calculation Methods

Most of the simulation methods used here were the same as those used in the previous investigation.<sup>2</sup> The film cooling model was new. The main features and the new procedures are introduced here.

#### 1. Engine Components and Working Fluids

The simulation used a quasi-one-dimensional method. In the external nozzle, combustion gas was assumed to flow with Prandtl-Meyer expansion. The kinetic energy efficiency of the inlet was 0.98. The engine thrust was calculated with integration of wall pressure, subtracting the friction drag.

Fluids in the engine, i.e., air, hydrogen, and the combustion product were calorically perfect gases. In order to simplify the simulation calculation in this model, there was no dissociation. The flow was viscous, and friction existed in the combustor/internal nozzle and in the cooling tubes.

Only the combustor/internal nozzle was cooled in this model; it can represent the cooling characteristics of the engine because the heat load of the engine is mainly imposed in the combustor/internal nozzle.<sup>25</sup> The combustor/internal nozzle was divided into a hundred elements, each element being composed of two parts, i.e., 1) the divergent part where the combustion gas expanded isentropically, and 2) the constant cross-sectional part where heat exchange and friction occurred. Reynolds analogy was used in calculation of heat

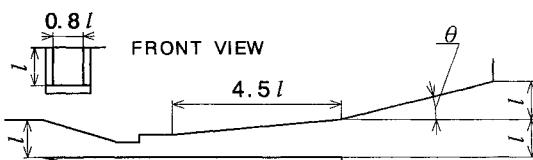


Fig. 6 Model engine configuration.

transfer, and Prandtl number was unity. The friction coefficient in the combustor/internal nozzle was calculated with van Driest's formula,<sup>26</sup> whereas the coefficient in the cooling tubes was calculated with the universal resistance law for smooth pipes.<sup>27</sup>

According to our previous investigation,<sup>2</sup> suitable material for a regeneratively cooled scramjet has high thermal conductivity, e.g., copper. So, the combustor/internal nozzle of the regeneratively cooled engine was made of copper. In the film cooled engine, a good engine wall material has high allowable temperature. Thus, zirconia<sup>28</sup> was used for the engine. In the engine with a combination of film cooling and regenerative cooling, copper was also used because it was cooled regeneratively and because the engine performances can be easily compared with those of the regeneratively cooled engine.

#### 2. Film Cooling

The film coolant was injected at a Mach number of 1.2. The static pressure of the coolant at the exit of the injection slot was the same as that of the main flow. The features of the film cooling were calculated utilizing the properties of the main flow and the coolant at the exit of the coolant injection slot. Average properties of the combustion gas flow were calculated using the mixture of the coolant and the main flow. Tendencies of performances of the film cooled engine were obtained through the present simulation because of the simplicity of the film cooling model and the simple integrity of the model to the flow simulation.

## IV. Simulation Results

Figure 7 shows the fuel flow rate of each engine as a form of equivalence ratio. The flow rate of the film cooled engine was one-tenth the value in the figure, extraordinarily high. Rates once decreased, then increased due to a combination of static pressure at the slot exit and heat load. The flow rate of the regeneratively cooled engine was stoichiometric at the low flight Mach numbers and increased with the flight Mach number at the high Mach numbers, being roughly proportional to 2.2 power of the flight Mach number.<sup>1</sup> The dotted line shows the cooling requirement of the regeneratively cooled engine at low flight Mach numbers. The fuel flow rate of the engine with a combination of film cooling and regenerative cooling was approximately stoichiometric, even at high Mach numbers.

When the growth rate of the mixing layer of the film coolant doubled, or when the power coefficient of the film cooling efficiency was set at  $-2$  instead of  $-0.8$  in the simulation with a combination of film cooling and regenerative cooling, the coolant flow rates were 1.19 and 1.24 of the equivalence ratios, respectively, at a flight Mach number of 24. The value of  $-2$  was selected because of the experimental datum shown in Fig. 4. Therefore, even though the present film cooling model cannot predict point  $x_A$ , nor the decline of the film cooling efficiency exactly, the combination of film cooling and

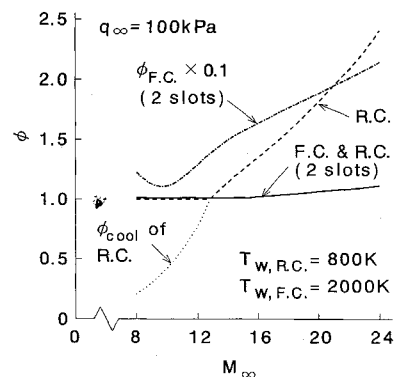


Fig. 7 Fuel flow rate.

regenerative cooling must be very effective in reducing the coolant flow rate.

Figure 8 shows the fuel supply pressure of each cooling system. The pressure losses of fuel were due to heat addition and due to friction in the cooling tubes. These losses did not include pressure losses in manifolds nor in bends. The required fuel supply pressure of the regeneratively cooled engine increased with the flight Mach number. This was due to the increment of heat load and that of fuel flow rate. The high pressure at low flight Mach numbers was due to the high fuel flow rate. On the other hand, the pressure of the engine with a combination of film cooling and regenerative cooling decreased with the flight Mach number. This was because the fuel flow rate decreased with the flight Mach number.

The high pressure in an engine requires a strong structure, e.g., a very thick engine wall. This results in a heavy engine. At the same time, the high pressure of fuel requires a fuel supply pump with high power. For example, when a gas generator cycle is adopted for the engine, the high power causes the turbine flow rate to increase. Since the exhaust velocity of the working gas of the turbine is usually small and the gas generator consumes oxidizer, the net specific impulse of the engine becomes low.<sup>4</sup> When the combined film and regenerative cooling techniques are adopted, the engine does not require high pressure of fuel, as seen in Fig. 8, and does not suffer a serious decrease of net specific impulse.

Figure 9 shows the net specific impulse of each engine. The contribution of the exhaust gas of the turbine mentioned above is not included. The specific impulse of the engine with only film cooling was very low due to the extraordinarily high fuel flow rate. The specific impulse of the regeneratively cooled engine became worse at high flight Mach numbers in comparison with that of the engine with a combination of film cooling and regenerative cooling. This was due to the increment of fuel flow rate as shown in Fig. 7. There was little difference of specific impulse between the engine with a combination of film cooling and regenerative cooling and the engine with a stoichiometric fuel flow rate.

Other advantages by film cooling, i.e., reduction of friction and augmentation of thrust, were observed in the simulation. Their effects on the specific impulse were, however, much smaller than the effect of the reduction of excess fuel at high flight Mach numbers.

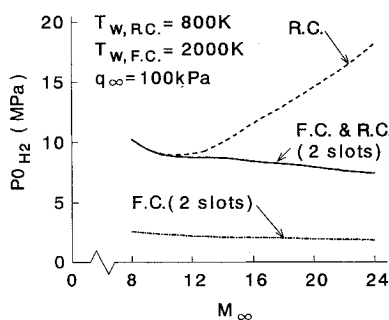


Fig. 8 Fuel supply pressure.

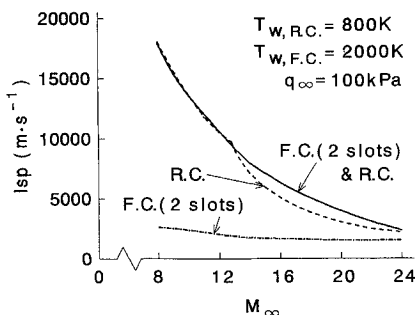


Fig. 9 Specific impulse.

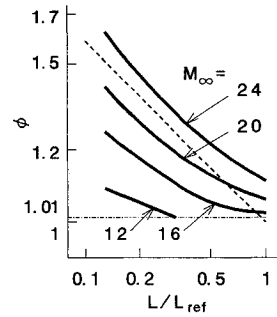


Fig. 10 Scale effect. The broken line shows the decline of  $-0.2$ .

Performances of the engine with a combination of film cooling and regenerative cooling were compared among three engines with different engine wall materials, i.e., copper, nickel alloy, and zirconia. Their maximum allowable temperatures were set at 800, 1000, and 2000 K, respectively. The copper engine showed the greatest fuel flow rate, and the zirconia engine showed the smallest. All the fuel flow rates of the three engines were in close proximity of stoichiometric flow rate, and there were slight differences in specific impulse among them. That of the zirconia engine was the best of the three.

In the development of a scramjet engine, a subscale model is to be tested first. Therefore, the scale effect was investigated. Figure 10 shows the fuel flow rate of the engine with a combination of film cooling and regenerative cooling. The configuration of the engine was proportional to the original one, i.e., the engine that had a cross section of 6 m<sup>2</sup> at the inlet entrance; the subscript "ref" represents this engine. As the engine became smaller, the thermal load became larger,<sup>1</sup> but the fuel flow rate was still small, compared with that of the regeneratively cooled engine.<sup>1</sup> The coolant flow rate was roughly proportional to the  $-0.2$  power of the representative length.

## V. Discussion

### A. Reduction of Coolant

In the engine with a combination of film cooling and regenerative cooling, there was a reduction of coolant flow rate. In this section, causes of the reduction are discussed.

#### 1. Effect of Coolant Temperature

The required flow rate of film coolant can be expressed as follows with Eq. (8):

$$\begin{aligned} \dot{m}_c &= l h p_c u_c \\ &= \underbrace{l x_1 \rho_c u_c}_{(a)} \underbrace{\frac{1}{2} \frac{d\delta}{dx} \left( \frac{T_{0m} - T_{aw,1}}{T_{0m} - T_{0c}} \right)^{5/4}}_{(b)} \end{aligned} \quad (9a)$$

$$\begin{aligned} &= \underbrace{l x_1 \rho_c M_c \sqrt{1 + [(\gamma_c - 1)/2] M_c^2} \sqrt{(\gamma_c/R_c T_{0c})}}_{(a)} \\ &\quad \times \underbrace{\frac{1}{2} \frac{d\delta}{dx} \left( \frac{T_{0m} - T_{aw,1}}{T_{0m} - T_{0c}} \right)^{5/4}}_{(b)} \end{aligned} \quad (9b)$$

Figure 11 shows the relation between required flow rate and total temperature of the film coolant in a sample cylindrical engine. Circumferential length of the engine  $l$  was 3.5 m, and the combustor length  $x_1$ , was 5 m. The film coolant was injected at sonic velocity parallel to the combustion gas. These operating conditions roughly correspond to those at a

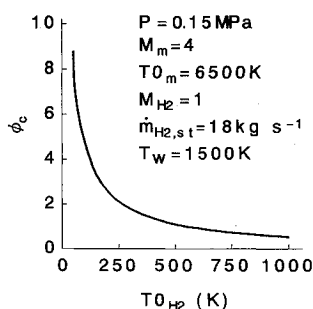


Fig. 11 Relation between flow rate and total temperature of film coolant.

flight Mach number of 14 and a flight dynamic pressure of 100 kPa.

The coolant flow rate decreased with increment of the total temperature. In the engine with a combination of film cooling and regenerative cooling, the film coolant was also heated. There are two mechanisms due to increment of the total temperature of the film coolant to reduce the required coolant flow rate. One is due to the height of the injection slot, as seen in Eq. (8). The height increases with an increase of volume flow rate, i.e., an increase of total temperature of the coolant at a specified coolant mass flow rate. The effect is expressed as a mass flux term in Eqs. (9a) and (9b) with (a). The term  $\rho_c \cdot u_c$  decreases with increment of total temperature. Even if point  $x_A$  in Fig. 1 was estimated in another way, this effect of the increased volume flow rate would be effective, i.e., the coolant flow rate would decrease with heating of the coolant.

The other mechanism is due to the velocity increment of the coolant. When the total temperature increases, velocity of the coolant increases at a specified injection Mach number. As the velocity difference between main flow and the coolant decreases, growth rate of the mixing layer, indicated in Eq. (9a) with (b), decreases. As for the compressibility effect, the convective Mach number was beyond unity in every simulation, and the value of  $f$  in Eq. (1) was always very close to 0.2 in the simulation. The part of growth rate dependent on incompressibility decreases with increment of total temperature of the film coolant as can be seen in Eq. (5b). So the increment of the total temperature is effective for reduction of coolant flow rate. The above two mechanisms were at the same order of effectiveness in Fig. 11. Film coolant must be used at high temperature to reduce its mass flow rate.

In this film cooling model, the static pressure at the film cooling injector exit has to be set at the pressure of the main flow, and the increment of the injection Mach number of the coolant increases the coolant flow rate. The general tendency of increment of the injection Mach number, therefore, cannot be investigated with this model.

No trouble should result from using hot hydrogen as coolant. Regarding film cooling, it has been reported that combustion was confined to the shear layer and maintained at a low level in experiments using air and hydrogen.<sup>9</sup> On the other hand, the fuel injected into the combustor will be stoichiometric or more, and the combustion gas will not contain any more oxygen than in average conditions. As for local conditions, part of the injected fuel will remain on the engine wall due to the imperfection of mixing. The hot film coolant, therefore, will not induce combustion.

## 2. System of Heat Exchange

In the engine with a combination of film cooling and regenerative cooling, there are other mechanisms for reduction of coolant mass flow rate in addition to the above-mentioned high-temperature effect. One is moderate cooling of the engine wall, and the other is shielding with coolant of the wall from the hot gas. In the engine with only film cooling, the wall temperature near the injection slot nearly reaches the

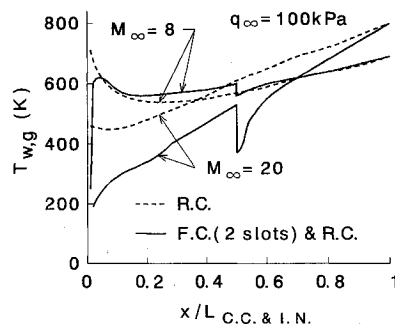


Fig. 12 Wall temperature of hot gas side in the quasi-one-dimensional simulation.

temperature of liquid hydrogen. The wall material does not need to be cooled to the temperature of liquid hydrogen, and a temperature around several hundred Kelvin is possible. In the engine with a combination of film cooling and regenerative cooling, the wall temperature near the slot was around several hundred Kelvin, as hot as the regeneratively heated hydrogen as shown in Fig. 12.

In the film cooled engine, the coolant shields the engine wall near the injection slot from the hot gas, the total temperature of which is around several thousand Kelvin at high flight Mach numbers. Heat load around the entrance of the combustor is greatest in the engine because of relatively high static pressure. Therefore, the largest heat load was avoided in the engine with a combination of film cooling and regenerative cooling, and the heat transfer to the regenerative coolant was much lower in this engine than in the engine with only regenerative cooling.

## B. Engine Wall Material

In the regeneratively cooled scramjet, engine wall material must have high thermal conductivity because of the much higher adiabatic wall temperature of the combustion gas than the maximum allowable temperature of the materials.<sup>2</sup> In the film cooled scramjet, the adiabatic wall temperature was much lower around the coolant injection slot than in the regeneratively cooled engine as mentioned above. It was still lower in the other region than in the regeneratively cooled engine. So, the increment of the allowable temperature of the material can reduce heat flux from the gas on the wall.

## C. Scale Effect

In the engine with a combination of film cooling and regenerative cooling, most of the engine wall was cooled regeneratively. Based on Fig. 1, it can be anticipated, where the length and the film cooling efficiency are plotted with logarithm scales. Thus, the coolant flow rate was roughly proportional to the  $-0.2$  power of the representative length, as in the regeneratively cooled engine.<sup>1</sup>

As for film cooling, the coolant flow rate is proportional to the squares of the representative length as shown in Eq. (9a), whereas the stoichiometric flow rate is also proportional to the squares of the length. The scale effect will not appear in the film cooling. The region was small where the film cooling was dominant, so the effect of the film cooling did not appear on the inclination of lines. In the vicinity of 1.01 of the equivalence ratio, the film cooling effect appeared, and the inclination of the lines became gentle.

## VI. Conclusions

A new film cooling model was introduced. It is based on experimental results on the compressible mixing layer and on the analysis using the turbulent boundary layer. It was applied to a quasi-one-dimensional simulation of a scramjet engine. The investigation clarified some aspects as follows:

1) There is the potential benefit in using a combination of film cooling and regenerative cooling to achieve thermal pro-

tection while minimizing fuel flow requirements, i.e., maintaining adequate specific impulse.

2) There are four mechanisms that reduce the coolant flow rate, i.e., a) decrease of growth rate of the mixing layer, b) increase of the volume flow rate of the coolant, c) avoidance of too much cooling of the wall about the temperature of liquid hydrogen, and d) shielding of the engine wall from the hot gas. a and b were realized by an increase of total temperature of the film coolant. c and d were realized by a combination of film cooling and regenerative cooling.

3) The reduction of excessive fuel flow rate also decreases the system pressure in the engine with a combination of film cooling and regenerative cooling at high flight Mach numbers. This makes the engine lighter. At the same time, it improves the net engine specific impulse due to the reduction of turbine power.

4) The coolant flow rate is roughly proportional to the  $-0.2$  power of a representative length in the engine with a combination of film cooling and regenerative cooling.

The film cooling model herein reported should be more fully developed and its consistency confirmed by further experiments and numerical simulations.

### Acknowledgment

The authors would like to thank N. Chinzei of the National Aerospace Laboratory for useful advice.

### References

- <sup>1</sup>Kanda, T., Masuya, G., Wakamatsu, Y., Chinzei, N., and Kanmuri, A., "Parametric Study of Airframe-Integrated Scramjet Cooling Requirement," *Journal of Propulsion and Power*, Vol. 7, No. 3, 1991, pp. 431-436.
- <sup>2</sup>Kanda, T., Masuya, G., and Moro, A., "Analytical Investigation of a Regeneratively Cooled Scramjet Engine," AIAA Paper 93-0739, Jan. 1993.
- <sup>3</sup>Scotti, S. J., Martin, C. J., and Lucas, S. H., "Active Cooling Design for Scramjet Engines Using Optimization Methods," AIAA Paper 88-2265, April 1988.
- <sup>4</sup>Kanda, T., Masuya, G., Wakamatsu, Y., Chinzei, N., and Kanmuri, A., "A Comparison of Scramjet Engine Performances Among Various Cycles," AIAA Paper 89-2676, July 1989.
- <sup>5</sup>Schetz, S. J., and Van Overeem, J., "Skin Friction Reduction by Injection Through Combinations of Slots and Porous Sections," *AIAA Journal*, Vol. 13, No. 8, 1975, pp. 971, 972.
- <sup>6</sup>Kamath, P., Baker, N., and McClinton, C., "A Computational Design Tool for Scramjet Combustor Film Cooling and Fuel Mixing Predictions," AIAA Paper 90-0645, Jan. 1990.
- <sup>7</sup>Kwok, F. T., Andrew, P. L., Ng, W. F., and Schetz, J. A., "Experimental Investigation of a Supersonic Shear Layer with Slot Injection of Helium," *AIAA Journal*, Vol. 29, No. 9, 1991, pp. 1426-1435.
- <sup>8</sup>Goldstein, R. J., Eckert, E. R. G., Tsou, F. K., and Haji-Seikh, A., "Film Cooling with Air and Helium Injection Through a Rearward-Facing Slot into a Supersonic Air Flow," *AIAA Journal*, Vol. 4, No. 6, 1966, pp. 981-985.
- <sup>9</sup>Bass, R., Hardin, L., and Rodgers, R., "Supersonic Film Cooling," AIAA Paper 90-5239, Oct. 1990.
- <sup>10</sup>Olsen, G. C., Nowak, R. J., Holden, M. S., and Baker, N. R., "Experimental Results for Film Cooling in 2-D Supersonic Flow Including Coolant Delivery Pressure, Geometry, and Incident Shock Effects," AIAA Paper 90-0605, Jan. 1990.
- <sup>11</sup>Holden, M. S., Nowak, R. J., Olsen, G. C., and Rodriguez, K. M., "Experimental Studies of Shock Wave/Wall Jet Interaction in Hypersonic Flow," AIAA Paper 90-0607, Jan. 1990.
- <sup>12</sup>Parthasarathy, K., and Zakkay, V., "An Experimental Investigation of Turbulent Slot Injection at Mach 6," *AIAA Journal*, Vol. 8, No. 7, 1970, pp. 1302-1307.
- <sup>13</sup>Hartnett, J. P., Birkebak, R. C., and Eckert, E. R. G., "Velocity Distributions, Temperature Distributions, Effectiveness and Heat Transfer for Air Injected Through a Tangential Slot into a Turbulent Boundary Layer," *Journal of Heat Transfer*, Vol. 83, No. 3, 1961, pp. 293-306.
- <sup>14</sup>Stollery, J. L., and El-Ehwany, A. A. M., "A Note on the Use of a Boundary-Layer Model for Correlating Film-Cooling Data," *International Journal of Heat and Mass Transfer*, Vol. 8, 1965, pp. 55-65.
- <sup>15</sup>Hatch, J. E., and Papell, S., "Use of a Theoretical Flow Model to Correlate Data for Film Cooling or Heating an Adiabatic Wall by Tangential Injection of Gases of Different Fluid Properties," NASA TN D-130, Nov. 1959.
- <sup>16</sup>Chinzei, N., Masuya, G., Komuro, T., Murakami, A., and Kudou, K., "Spreading of Two-Stream Supersonic Turbulent Mixing Layers," *Physics of Fluids*, Vol. 29, No. 5, 1986, pp. 1345-1347.
- <sup>17</sup>Papamoschou, D., and Roshko, A., "The Compressible Turbulent Shear Layer: An Experimental Study," *Journal of Fluid Mechanics*, Vol. 197, 1988, pp. 453-477.
- <sup>18</sup>Dimotakis, P., "Turbulent Free Shear Layer Mixing and Combustion," *Proceedings of the 9th International Symposium on Air Breathing Engines*, AIAA, Washington, DC, 1989, pp. 58-79.
- <sup>19</sup>Culick, F. E. C., and Hill, J. A., "A Turbulent Analog of the Stewartson-Illingworth Transformation," *Journal of Aeronautical Sciences*, Vol. 25, No. 4, 1958, pp. 259-262.
- <sup>20</sup>Seban, R. A., "Heat Transfer and Effectiveness for a Turbulent Boundary Layer with Tangential Fluid Injection," *Journal of Heat Transfer*, Vol. 82, No. 4, 1960, pp. 303-312.
- <sup>21</sup>Seban, R. A., and Back, L. H., "Velocity and Temperature Profiles in Turbulent Boundary Layers with Tangential Injection," *Journal of Heat Transfer*, Vol. 84, No. 1, 1962, pp. 45-54.
- <sup>22</sup>Clark, R. L., Jr., Ng, W. F., Walker, D. A., and Schetz, J. A., "Large-Scale Structure in a Supersonic Slot-Injected Flowfield," *AIAA Journal*, Vol. 28, No. 6, 1990, pp. 1045-1051.
- <sup>23</sup>Zhuang, M., Kubota, T., and Dimotakis, P., "Instability of Inviscid, Compressible Free Shear Layers," *AIAA Journal*, Vol. 28, No. 10, 1990, pp. 1728-1733.
- <sup>24</sup>Abe, T., Funabiki, K., Ariga, H., and Hiraoka, K., "Effect of Streamwise Pressure Gradient on the Supersonic Mixing Layer," *AIAA Journal*, Vol. 30, No. 10, 1992, pp. 2564-2566.
- <sup>25</sup>Kanda, T., Masuya, G., and Wakamatsu, Y., "Propellant Feed System of a Regeneratively Cooled Scramjet," *Journal of Propulsion and Power*, Vol. 7, No. 3, 1991, pp. 299-301.
- <sup>26</sup>White, F. M., *Viscous Fluid Flow*, McGraw-Hill, New York, 1974, p. 639.
- <sup>27</sup>Schlichting, H., *Boundary Layer Theory*, 7th ed., McGraw-Hill, New York, 1979, p. 610.
- <sup>28</sup>Sutton, G. P., and Ross, D. M., *Rocket Propulsion Elements*, 4th ed., Wiley, New York, 1976, p. 117.